

PAPER

## The effect of the direct current electric field on the dynamics of the ultracold plasma

To cite this article: Syed ZAHEERUDDIN *et al* 2018 *Plasma Sci. Technol.* **20** 085001

View the [article online](#) for updates and enhancements.

### Related content

- [Ultracold neutral plasmas](#)  
M Lyon and S L Rolston
- [Ultracold neutral plasmas: recent experiments and new prospects](#)  
T C Killian, V S Ashoka, P Gupta *et al.*
- [Using sheet fluorescence to probe ion dynamics in an ultracold neutral plasma](#)  
J Castro, H Gao and T C Killian

# The effect of the direct current electric field on the dynamics of the ultracold plasma

Syed ZAHEERUDDIN<sup>1,2</sup>, Yufan LI (李煜璠)<sup>1,2</sup>, Dongmei ZHAO (赵冬梅)<sup>1</sup>,  
Xinwen MA (马新文)<sup>1</sup> and Jie YANG (杨杰)<sup>1</sup>

<sup>1</sup>Institute of Modern Physics, Chinese Academy of Sciences, Lanzhou 730000, People's Republic of China

<sup>2</sup>University of Chinese Academy of Sciences, Beijing 100049, People's Republic of China

E-mail: [jie.yang@impcas.ac.cn](mailto:jie.yang@impcas.ac.cn)

Received 14 March 2018, revised 23 April 2018

Accepted for publication 24 April 2018

Published 6 July 2018



CrossMark

## Abstract

We created an ultracold plasma by photoionizing the laser-cooled and trapped rubidium atoms in a magneto-optical trap. In the externally applied direct current (DC) electric field environment, the electrons which escape from the potential well of the ultracold plasma were detected for different numbers of the ions and initial kinetic energies of the electrons. The results are in good agreement with the calculations, based on the Coulomb potential well model, indicating that the external DC field is an effective tool to adjust the depth of potential well of the plasma, and it is possible to create an ultracold plasma in a controlled manner.

Keywords: ultracold plasma, magneto-optical trap, photoionization, Coulomb potential well model

(Some figures may appear in colour only in the online journal)

## 1. Introduction

The development of laser cooling and trapping of neutral atoms [1] opened new windows for many physical research fields, including atomic, optical, and plasma physics. The study of ultracold plasma based on the cold atoms is one of the state-of-the-art topics in the field of low-temperature plasma physics. In the ultracold plasma, the Coulomb interaction energy between nearest neighbors exceeds the thermal energy of the charged particles, making it strongly coupled plasma [2]. The Coulomb coupling parameter,  $\Gamma$ , one of the most important parameters in the field of plasma physics, is defined as the ratio of the electrostatic energy to the thermal energy

$$\Gamma = \frac{e^2}{4\pi\epsilon_0 a k_B T} \quad (1)$$

with  $a = (3/4\pi n)^{1/3}$  is the Wigner–Seitz radius,  $e$  is the electron charge,  $k_B$  is the Boltzmann's constant,  $n$  and  $T$  are the number density and the temperature of the particles in the plasma, respectively. The strongly coupled plasmas usually exist in astrophysical environments with very high density and high temperature, such as quark-gluon plasmas, the Mott-insulator transition, non-neutral and dusty plasmas [3–11]. Strong coupling effect can also be found in high density

artificial plasmas, for example, laser-produced plasma and laser-driven fusion plasma [12]. However, due to the extremely high temperatures and densities, it is very difficult to study the dynamics of these plasmas directly. The ultracold plasmas, however, allow the formation of strongly coupled plasmas at low densities and controllable initial conditions in the laboratory.

So far, many experiments, as well as many theoretical and computational calculations and simulations, have investigated the dynamics of ultracold plasma in different conditions [13–26]. The time-dependent properties of the ultracold plasma, including the temperatures and the densities of charged particles, are very important to the study of the evolution of the ultracold plasma. In 1999, Killian *et al* [13] introduced the Coulomb potential well model to understand the formation and evolution of ultracold plasma. Then, many experimental works investigated the relations of the key parameters in the model, such as the threshold number of the ions, size of the plasma, and the effective electric field [27–32]. The effective electric field in the Coulomb potential well model can be tunable by an applying an external electric field. However, no experimental results have been reported so far concerning the effect of the direct current (DC) electric field on the dynamics of the ultracold plasma.

In the present study, we created ultracold plasma by photoionizing the laser-cooled rubidium (Rb) atoms in a magneto-optical trap (MOT). In the externally applied DC electric field environment, the electrons which escape from the potential well of the ultracold plasma were detected for different numbers of ions and initial kinetic energies of electrons. The magnitude of DC field was tuned to adjust the depth of the potential well of the plasma. In addition, the Coulomb potential well model was used to calculate and explain the dynamics of the ultracold plasma.

## 2. Experimental setup

The details of the experimental setup have been described in [33]. Briefly, about  $10^7$   $^{87}\text{Rb}$  atoms with a typical temperature of  $500\ \mu\text{K}$  are prepared in a MOT. The spatial distribution of the cold atoms cloud is Gaussian with a diameter of  $1.4\ \text{mm}$  and the corresponding peak density of about  $10^{10}\ \text{cm}^{-3}$ . The cold atoms are photoionized using two-step scheme. In the first step, the atoms are excited from  $5^2\text{S}_{1/2}(F=2)$  state to  $5^2\text{P}_{3/2}(F'=3)$  state by a diode laser (Toptica DL 100) with a wavelength of  $780\ \text{nm}$ , which is also the cooling circle for the MOT. In the second step, the atoms in  $5^2\text{P}_{3/2}(F'=3)$  state are photoionized by a pulsed Nd:YAG laser pumped dye laser (Sirah Cobra-Stretch,  $10\ \text{Hz}$  and  $5\ \text{ns}$ ) which is focused on the cold atoms with a waist of  $250\ \mu\text{m}$ . The wavelength of the dye laser is tunable above the ionization potential of  $^{87}\text{Rb}$  atom from  $1$  to  $1000\ \text{cm}^{-1}$ . The status of the cold atoms, including the temperature and the density, is monitored by the fluorescence detector, and the number of ions is estimated from the loss of the fluorescence.

Ten pairs of parallel electrodes are placed near the cold atom cloud to extract electrons from the plasma and accelerate them to a microchannel plate (MCP) detector by applying an external DC voltage. The magnitude of the DC electric field is tunable in the range of  $35\text{--}350\ \text{mV cm}^{-1}$ . In the DC field environment, the ions and electrons produced by the photoionization play a two-fold role. First, a small part of electrons is removed by the DC field, and the corresponding ions are nearly immobile and create a counterbalance electric field for the external DC field. Second, the remaining part of the ions and electrons creates a Coulomb potential well, and forms an ultracold plasma. Hence, the DC field can adjust the number of ions/electrons in the ultracold plasma, that is, tune the depth of the Coulomb potential well of the ultracold plasma.

The signals from the detectors are converted to digital signals by a fast A/D converter (Pico Scope 6404D) with  $500\ \text{MHz}$  bandwidth and  $12$  bits dynamic range, then recorded by a computer. The time references for different apparatus are provided by two synchronized pulse generators (Stanford Research Systems DG645).

## 3. Results and discussion

### 3.1. Creation and detection of the ultracold plasma in the DC field

As mentioned above, cold  $^{87}\text{Rb}$  atoms in  $5^2\text{P}_{3/2}(F'=3)$  state are photoionized by a pulsed dye laser to create the ultracold

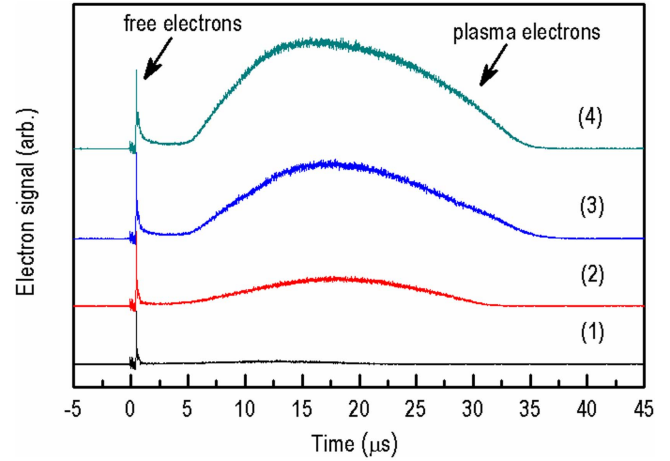


**Figure 1.** Electron signals recorded for four different energies of the pulsed dye laser: (1)  $4.3\ \mu\text{J}$ , (2)  $13.6\ \mu\text{J}$ , (3)  $43\ \mu\text{J}$ , and (4)  $136\ \mu\text{J}$ . The laser wavelength is about  $6\ \text{cm}^{-1}$  above the ionization potential of Rb atom, so the initial electron temperature is about  $10\ \text{K}$ . The photoionization occurs at  $t = 0\ \mu\text{s}$ . The magnitude of external DC electric field is  $35\ \text{mV cm}^{-1}$ . The experiment is repeated 100 times for each spectrum.

plasma. The available energy to the plasma is the difference between photon energy and the ionization potential of  $^{87}\text{Rb}$ ,  $\Delta E = h\nu - E_{\text{IP}}$ . The momentum conservation can be written as

$$p_e \approx -p_i \quad (2)$$

and the energy conservation can be expressed as

$$\Delta E = \frac{p_i^2}{2m_i} + \frac{p_e^2}{2m_e} = \left(1 + \frac{m_i}{m_e}\right) \frac{p_i^2}{2m_i} \quad (3)$$

so the kinetic energies of electrons and ions are approximately

$$E_e \approx \Delta E \text{ and } E_i \approx \frac{m_e}{m_i} \Delta E. \quad (4)$$

Due to the large ion to electron mass ratio, the ions are nearly immobile on the time scale of photoionization, and the excess energy is almost taken away by the electrons. As a result, some of the free electrons escape from the cloud, and the external DC field directs the escaped electrons towards the detector, which produce the first sharp peak signals as shown in figure 1.

The remaining cloud is positively charged, which forms an attractive Coulomb potential well for the next electrons trying to leave the cloud. From [13], the corresponding Coulomb potential energy is expressed as

$$U = \sqrt{\frac{2}{\pi}} \frac{N_i e^2}{4\pi\epsilon_0\sigma}, \quad (5)$$

where  $U$  is the Coulomb potential, and  $N_i$  is the number of ions that have a Gaussian density distribution of characteristic size  $\sigma$ . The more the electrons escape, the more the potential well deepens. Once the well depth equals the electron kinetic energy, no more electrons escape, and hence the ultracold plasma is formed. The relevant number of ions is called the threshold ion number [13]. The trapped electrons in the

potential well exert an outward pressure on the ions that causes an expansion in the plasma cloud. For a self-similar expansion, the characteristic size of the ultracold plasma would follow  $\sigma(t) = \sqrt{\sigma(0)^2 + v^2 t^2}$ , where  $\sigma(0)$  is the initial size of the ultracold plasma,  $v$  is the asymptotic expansion velocity and given by  $v = \sqrt{2\Delta E/3m_i}$ . As a result, the plasma finally expands into the vacuum with a velocity of the order of  $100 \text{ m s}^{-1}$  [32, 34]. With the expansion of the plasma, the ion density decreases, and the potential well gets shallower. So the trapped electrons escape from the plasma, guided by the applied DC field towards the MCP detector, and form the second peaks as shown in figure 1.

The electron signals recorded for four different dye laser energies, which correspond to the initial numbers of ions/electrons produced in photoionization, are shown in figure 1. At low laser energy, the number of created ions is not enough to form plasma, as a result, the second peak intensity is almost invisible. With the increase in laser energy, the number of ions exceeds the threshold, the potential well deepens, and the plasma signals are seen [13]. Kulin *et al* [16] reported that when the initial electron kinetic energy is above 10 K, the plasma expansion follows a simple hydrodynamic electron pressure model. This model describes the expansion of a single-component cloud of non-interacting particles at temperature  $T_e$ , as a result, the lifetime of the plasma does not change significantly. As shown in figure 1, the contours and the time properties of the plasma signals in different laser energies are very similar, showing a similar lifetime and behavior of ultracold plasma as described in the hydrodynamic model.

### 3.2. Ultracold plasma with different initial electron kinetic energies

The initial electron kinetic energy plays an important role in the formation of ultracold plasma [13, 32]. In this section, we investigated the behavior of ultracold plasma with different initial electron kinetic energies which experimentally controlled by the wavelength of the pulsed dye laser.

Figure 2(a) shows the electron signals for different initial electron kinetic energies. On increasing the initial electron kinetic energy, the free electron signal increases and the plasma signal becomes sharp and moves gradually towards the shorter time, meaning that the lifetime of the plasma becomes shorter. Qualitatively, the lifetime of the plasma is dominated by the plasma expansion. From the hydrodynamic model, the electrons with high initial kinetic energy will drive the plasma expansion faster and shorten the lifetime of the plasma.

The plasma signals in figure 2(a) are integrated to get the numbers of trapped electrons for different initial electron kinetic energies as shown in the figure 2(b). The number of trapped electrons decreases with increasing initial electron kinetic energy. On one hand, the electrons with higher initial kinetic energy require deeper potential well to form ultracold plasma, so larger part of the electrons is lost to deepen the Coulomb potential well. On the other hand, the electrons with higher initial kinetic energy are relatively easier to escape

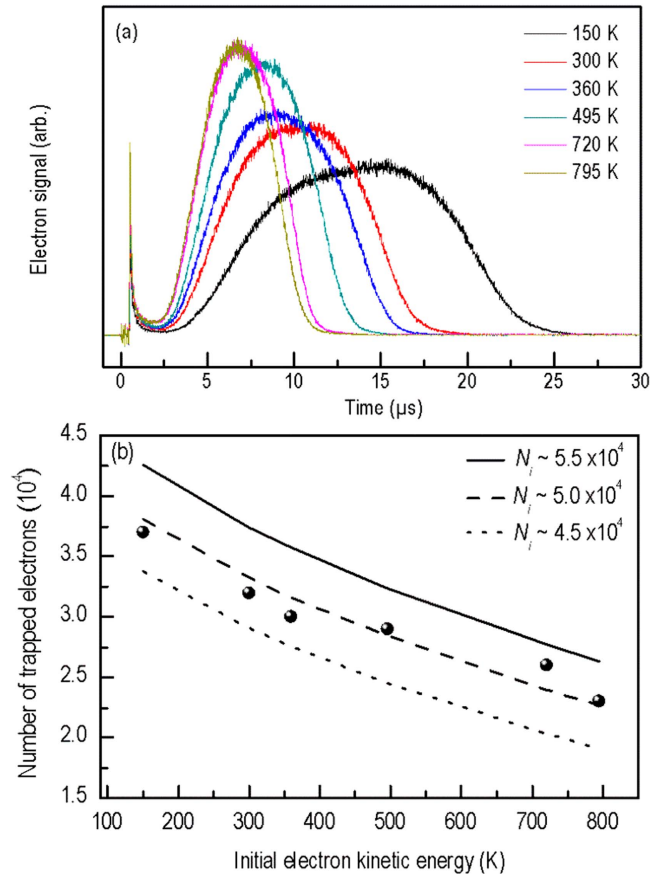


**Figure 2.** (a) Electron signals for different initial electron kinetic energies. The wavelength of the dye laser is tuned above the ionization potential of Rb from 100 to 600  $\text{cm}^{-1}$ , and the corresponding initial electron temperatures are displayed. The magnitude of external DC electric field is  $35 \text{ mV cm}^{-1}$ . (b) The number of trapped electrons for the different initial electron kinetic energies. The measured data are shown as circles, and the solid, dashed and dotted lines correspond to the calculations using the Coulomb potential well model.

from the trap, and as a result, a small fraction of electrons is trapped.

Based on the Coulomb potential well model, the number of trapped electrons ( $N_e$ ) as a function of both the number of ions ( $N_i$ ) and the threshold number of ions ( $N^*$ ) are shown as [13, 30]

$$N_e = N_i - \sqrt{N^* N_i}. \quad (6)$$

At the threshold condition, the potential well depth equals the electron kinetic energy, and the size of the system ( $\sigma$ ) equals to the Debye screening length ( $\lambda_D = \sqrt{\epsilon_0 k_B T_e / e^2 n_e}$ ), so equation (5) can be written as

$$N^* = \sqrt{\frac{\pi}{2}} \frac{4\pi\epsilon_0 \sigma E_e}{e^2}. \quad (7)$$

The threshold ion number is the minimum number of the ions required to trap electrons, in other words, the number of ions sufficient to create potential well, and grows linearly with increasing initial electron kinetic energy.

The calculated results are shown in figure 2(b), the solid, dashed, and dotted lines represent the number of ions which

correspond to 55 000, 50 000 and 45 000, respectively. With the increase in initial kinetic energy, the threshold value  $N^*$  increases, and the number of trapped electrons  $N_e$  decreases. It can be seen from figure 2(b) that the experimental results are in good agreement with the calculation in the condition where the number of ions is approximately equal to 50 000, indicating that the behavior of ultracold plasma follows the Coulomb potential well model. To keep on increasing the external DC field or the initial electron kinetic energy, all the electrons will escape, and no ultracold plasma will be formed. Therefore, trapping of electrons is very important for the formation of ultracold plasma. For a large fraction of trapped electrons, it is necessary to have a small size of the cloud, high density of charged particles, and low initial electron kinetic energy [27].

### 3.3. Ultracold plasma dependence on the DC field

As mentioned above, part of ions counterbalance the external DC field, so the  $N_i$  in equation (6) is the effective number of ions, which creates the potential well for the electrons and forms the ultracold plasma. In other words, the depth of Coulomb potential well of ultracold plasma is adjustable by the magnitude of the external DC field. Theoretically, the DC electric field,  $F$ , is given by the following expression [30]

$$F = \frac{e}{4\pi\epsilon_0} \frac{N_{i,v} - N_e}{\sigma(0)^2}, \quad (8)$$

where  $N_{i,v}$  is the number of photoions during photoionization. With the fixed number of photoions and an increase in the magnitude of the DC field, more ions are needed to counterbalance the DC field, and hence fewer ions/electrons are used to form the plasma.

In addition, the DC field is along one dimension, however, in the other two dimensions, the space charge effect from the counterbalance ions will be more significant with the increasing in the DC field. Vanhaecke *et al* [35] calculated the maximum electric field created by the ionic space charge, assuming that there are always a few electrons with zero velocity in the potential well, that is

$$F^{\text{th}} = \frac{V^{\text{th}}}{d} \approx 2.38 \frac{q_i}{4\pi\epsilon_0} n_i^0 \sqrt{2\sigma^2}, \quad (9)$$

where  $F^{\text{th}}$  and  $V^{\text{th}}$  are the threshold electric field and voltage, respectively, and  $n_i^0 = \frac{N_{i,v}}{(2\pi\sigma^2)^{3/2}}$  is the number density of the photoions.

Figure 3(a) shows the electrons signals for different magnitudes of the DC field with a fixed initial electron temperature of 10 K. In a low field, less number of electrons escape from the cloud, so there are enough electrons to be trapped in the potential well and form the plasma. On gradually increasing the DC field, the lifetime of the plasma shortens due to the space charge effect of the increasing counterbalance ions.

In figure 3(b), we show the number of trapped electrons as a function of the DC field magnitude. The circle represents the number of trapped electrons, which comes from the integration of the plasma signals in figure 3(a). The depth of

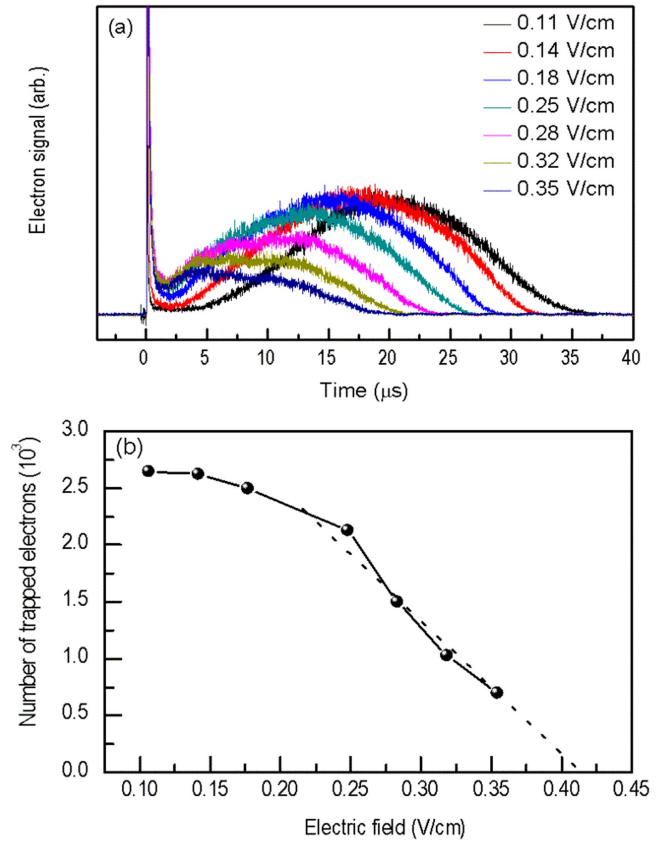


**Figure 3.** (a) Electron signals for different applied DC electric fields. The initial temperature of photoelectrons is about 10 K. The total number of ions is about  $5 \times 10^4$ . (b) The number of trapped electrons as function of the applied DC field. The extension of dotted line shows the cut-off point of the DC field at which the potential well is completely destroyed.

the potential well of the ultracold plasma is tuned by varying the magnitude of the DC field. When the DC field increases, the number of counterbalance ions increases, as a result, the number of trapped electrons decreases. To keep increasing the DC field, we can get the threshold DC field as shown in figure 3(b) by the extension of the dotted line at  $0.42 \text{ V cm}^{-1}$ . At the threshold DC field, all the trapped electrons are removed from the potential well, and hence the Coulomb potential well is completely destroyed. According to equation (8), the field produced by the photoions is about  $0.5 \text{ V cm}^{-1}$ , which is  $0.08 \text{ V cm}^{-1}$  higher than the experimental value, because that the space charge effect of the counterbalance ions drives the plasma expansion and decreases the field intensity. From another point of view, the threshold DC field equals the depth of the Coulomb potential well produced by the ions and electrons without any perturbation.

## 4. Conclusion

In conclusion, the ultracold plasma was created by the photoionization of the laser-cooled  $^{87}\text{Rb}$  atoms. The free electrons which escape from the potential well of the ultracold

plasma were detected in an external applied DC electric field. The behavior of the ultracold plasma was investigated for different numbers of ions and initial kinetic energies of electrons. In addition, the Coulomb potential well model was used to calculate and explain the dynamics of the ultracold plasma. The good match of experimental and theoretical results shows that it is possible to modify the formation and evolution of ultracold plasma by selecting the available experimental parameters, including the characteristic initial size of plasma, the wavelength and energy of ionization laser, and the magnitude of the external DC electric field.

## Acknowledgments

This work was supported by the National Key R&D Program of China (Grant No. 2017YFA0402300), National Natural Science Foundation of China (Grant No. 11404346), and the Strategic Priority Research Program of the Chinese Academy of Sciences (Grant No. XDB21030900). S Zaheeruddin is also grateful for the financial support of CAS-TWAS President's Fellowship Program for International PhD students.

## References

- [1] Metcalf H J and van der Straten P 2001 *Laser Cooling and Trapping* (New York: Springer)
- [2] Ichimaru S 1982 *Rev. Mod. Phys.* **54** 1017
- [3] van Horn H M 1991 *Science* **252** 384
- [4] Bathgate S N, Bilek M M M and McKenzie D R 2017 *Plasma Sci. Technol.* **19** 083001
- [5] Rischke D H 2004 *Prog. Part. Nucl. Phys.* **52** 197
- [6] Yin H, Efaaf M J and Zhang W 2012 *Plasma Sci. Technol.* **14** 445
- [7] Bourdel T et al 2004 *Phys. Rev. Lett.* **93** 050401
- [8] Spielman I B, Phillips W D and Porto J V 2007 *Phys. Rev. Lett.* **98** 080404
- [9] Kriesel J M et al 2002 *Phys. Rev. Lett.* **88** 125003
- [10] Liu B and Goree J 2008 *Phys. Rev. Lett.* **100** 055003
- [11] Hong Y et al 2017 *Plasma Sci. Technol.* **19** 055301
- [12] Murillo M S J 2009 *Phys. A: Math. Theor.* **42** 214054
- [13] Killian T C et al 1999 *Phys. Rev. Lett.* **83** 4776
- [14] Robinson M P et al 2000 *Phys. Rev. Lett.* **85** 4466
- [15] Pohl T, Pattard T and Rost J M 2003 *Phys. Rev. A* **68** 010703
- [16] Kulin S et al 2000 *Phys. Rev. Lett.* **85** 318
- [17] Killian T C et al 2001 *Phys. Rev. Lett.* **86** 3759
- [18] Fletcher R S, Zhang X L and Rolston S L 2007 *Phys. Rev. Lett.* **99** 145001
- [19] Simien C E et al 2004 *Phys. Rev. Lett.* **92** 143001
- [20] Cummings E A et al 2005 *Phys. Rev. Lett.* **95** 235001
- [21] Mazevet S, Collins L A and Kress J D 2002 *Phys. Rev. Lett.* **88** 055001
- [22] Robicieux F and Hanson J D 2002 *Phys. Rev. Lett.* **88** 055002
- [23] Kuzmin S G and O'Neil T M 2002 *Phys. Rev. Lett.* **88** 065003
- [24] Pohl T, Pattard T and Rost J M 2004 *Phys. Rev. A* **70** 033416
- [25] Niffenegger K, Gilmore K A and Robicieux F 2011 *J. Phys. B: At. Mol. Opt. Phys.* **44** 145701
- [26] Jinbo L et al 2014 *Plasma Sci. Technol.* **16** 305
- [27] Killian T C et al 2007 *Phys. Rep.* **449** 77
- [28] Lyon M and Rolston S L 2017 *Rep. Prog. Phys.* **80** 017001
- [29] Roberts J L et al 2004 *Phys. Rev. Lett.* **92** 253003
- [30] Comparat D et al 2005 *Mon. Not. R. Astron. Soc.* **361** 1227
- [31] Rezende D C J et al 2006 *Laser Phys.* **16** 1706
- [32] Wilson T, Chen W T and Roberts J 2013 *Phys. Plasma* **20** 073503
- [33] Li Y et al 2018 *J. Phys. Soc. Japan* **87** 054301
- [34] Rolston S L 2008 *Physics* **1** 2
- [35] Vanhaecke N et al 2005 *Phys. Rev. A* **71** 013416